



## Manufacturing and Characterization of Magnéli Phase Conductive Fibres

Journal:	<i>Journal of Materials Chemistry A</i>
Manuscript ID:	TA-ART-02-2014-000685.R1
Article Type:	Paper
Date Submitted by the Author:	16-Mar-2014
Complete List of Authors:	Bowen, Chris; Univ Bath, Materials Research Centre Adamaki, Vana; University of Bath, Pennock, Steve; U. Bath, Taylor, John; Univ Bath, Clemens, Frank; EMPA, Laboratory for High Performance Ceramics P.Ragulys, P.; Semiconductor Physics Institute,

## ARTICLE

## Manufacturing and Characterization of Magnéli Phase Conductive Fibres

Cite this: DOI: 10.1039/x0xx00000x

V. Adamaki<sup>a</sup>, F. Clemens<sup>b</sup>, P. Ragulis<sup>c</sup>, S. R. Pennock<sup>d</sup>, J. Taylor<sup>d</sup> and C. R. Bowen<sup>a</sup>

Received 00th January 2012,  
Accepted 00th January 2012

DOI: 10.1039/x0xx00000x

www.rsc.org/

This paper reports a simple and inexpensive method for preparing fine scale ( $\varnothing$  260  $\mu\text{m}$ ) and high-density Magnéli phase ( $\text{Ti}_n\text{O}_{2n-1}$ ) conductive ceramic fibres. The structure of the fibres was characterized by X-ray diffraction and scanning electron microscopy and their phase and microstructure related to frequency dependent impedance measurements. The process employed is capable of producing dense (>96%) Ti-sub oxides fibres and by using a reduction temperature of 1200°C and 1300°C it is possible to produce Magnéli phases fibres. The electrical conductivity of the reduced fibres can be tuned in a range of five orders of magnitude ( $10^{-1}$ - $10^4$  S/m) and the increase in conductivity was  $10^{13}$  relative to stoichiometric  $\text{TiO}_2$ . Such novel conductive fibres have the potential to be used as a sensing element, electrode, catalyst support and in energy storage applications.

### Introduction

As a n-type semiconductor due to the presence of oxygen vacancies,  $\text{TiO}_2$  has been studied in detail [1, 2] and used in a variety of technological applications such as in paints and food as a white pigment [3], orthopaedic and dental implants [4], catalyst supports [5, 6], photo-catalysis [7], photo-splitting of water [8,9,10] dye-sensitised solar cells [11] and gas-sensing [12]. While stoichiometric  $\text{TiO}_2$  has a low electrical conductivity of typically  $10^{-10}$  S/m, it is well known that its conductivity can be significantly increased by heat-treating the oxide at a high temperature in a reducing atmosphere [13]. The reduction process leads to the formation of sub-stoichiometric titanium oxides of the general formula  $\text{Ti}_n\text{O}_{2n-1}$  (with  $3 < n < 10$ ), known as Magnéli phases [1]. In non-stoichiometric titanium dioxide,  $\text{TiO}_{2-x}$ , with a low  $x$  ( $0 < x < 0.10$ ), the dominant point defects in the structure consist of  $\text{Ti}^{3+}$  and  $\text{Ti}^{4+}$  interstitials and oxygen vacancies [14]. However the Magnéli phases ( $x=0.10$ - $0.34$ ) are characterised by extended planar defects and crystallographic shear planes which vary according to the oxygen deficiency [15,16]. Due to their high electrical conductivity and chemical resistance, Magnéli phases are of interest in a variety of applications, which include cathodic protection, batteries, catalyst support for fuel cells as well as their potential use in the treatment of aqueous waste and contaminated water [13,17,18]. A comprehensive understanding of the transition of the conductive mechanism from insulating to semiconducting and eventually metallic is crucial in order to modify the electrical properties to meet the requirements of the above applications.

The majority of research on Magnéli phases materials has concentrated on the fabrication of bulk materials or powders [19, 20]. This paper describes a process to produce fine scale ( $\sim$ 250  $\mu\text{m}$ ) dense Magnéli phases fibres that enables the modification of the conductivity in a wide range. Such novel fibres can have use in applications such as sensing, catalysis [21] as a micro-electrode material [22,23] and energy storage [13, 24]. Understanding the

underlying structure of the conductive fibres formed and relating it to the electrical properties aids in developing fibre materials that meet the requirements of specific applications.

### Experimental methods

#### Fibre manufacture

Figure 1 is a schematic diagram of the process developed to create the Magnéli fibres. The  $\text{TiO}_2$  fibres were produced using a thermoplastic extrusion process. Titanium dioxide powder (PI-KEM, 99.5%, 0.3  $\mu\text{m}$  particle size, specific surface area 7.49  $\text{m}^2/\text{g}$ ) was pre-coated with three monolayers of stearic acid (93661, Fluka Chemie AG, Switzerland). The stearic acid was solved in toluene and mixed with the ceramic powder in a jar-mill with zirconia milling media for 12h. The toluene was dried out using a rotary evaporator (Rotavapor R-134, Büchi Labortechnik AG, Switzerland). The pre-mixed powder was blended with polyethylene binder (1700MN18C Lacqteme PEBD, Arkema Group, Cedex, France) using a torque rheometer (HAAKE PolyLab Mixer, Rheomix 600, Thermo Scientific, Karlsruhe, Germany). For the two-step mixing a temperature of 150°C (1<sup>st</sup> step) and 120°C (2<sup>nd</sup> step) was used. After mixing a thermoplastic homogeneous feedstock with 54 vol.% of  $\text{TiO}_2$  powder was achieved. This feedstock was used for thermoplastic extrusion of fibres with a diameter of 300  $\mu\text{m}$  using a capillary rheometer (RH7-2, Malvern, Herrenberg, Germany) at a temperature of 120°C.

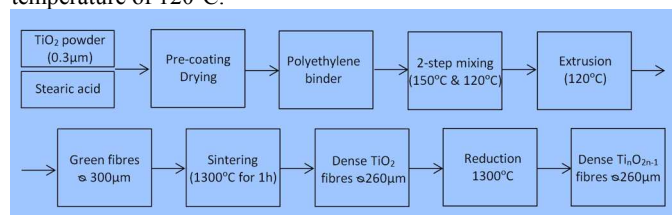
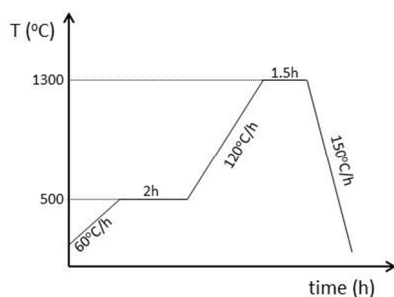


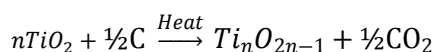
Figure 1. Process for forming Magnéli phase fibres.

A special ceramic die design (Empa, Switzerland) with an orifice of 300  $\mu\text{m}$  was used to produce the fibres. The fibres were extruded with a ram speed of 0.5 mm/s and a pressure of 13 MPa [25]. The 'green'  $\text{TiO}_2$  fibres were cut on a conveyor belt into 170 mm long pieces and the 'green-body' fibres were then sintered at 1300°C for 1.5h in chamber furnace (UAF, LENTON, UK) with a step at 500°C in order to burn out the binder (Figure 2). This sintering pattern was selected after optimization in order to achieve high-density fibre and to avoid a significant grain growth. After sintering the diameter of the  $\text{TiO}_2$  fibres was 260 $\mu\text{m}$ .



**Figure 2.** Sintering pattern for the dense  $\text{TiO}_2$  fibres.

To produce the Magnéli phases fibres the  $\text{TiO}_2$  sintered fibres initially sintered to high density were reduced through a carbo-thermal process,



performed in a tubular furnace (LTF, LENTON, UK), under constant Argon flow to avoid re-oxidation. After a number of trials, the optimal set up is to create a microenvironment, where the fibres are embedded in the carbon black powder, Figure 3. Table 1 shows the six different reduction treatments that were followed. These were selected based on initial experiments. For example, XRD of samples reduced at 1300°C for 1, 2, 4, 6 and 8 hrs, showed no difference in the phases present and to control grain growth in the fibres a 1hr of reduction at 1300°C was chosen (see Table 1). At lower reduction temperatures longer times were chosen due to the lower diffusion rates. In order to conduct density measurements, larger Magnéli phase tablets were prepared using the same thermal treatments.  $\text{TiO}_2$  powder was initially processed by adding 2.5wt.% of polyethylene glycole (PEG) 8000 molecular weight (MW) and distilled water to create a slurry which was ball-milled for 24 h, dried and sieved through a mesh (45  $\mu\text{m}$ ). Green-body pellets were formed by uniaxial pressing at 200 MPa. Typical sample dimensions were 10.6 mm diameter with a 1.3-1.4 mm thickness.

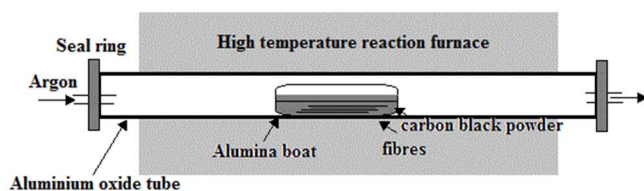


**Figure 3.** Setup and micro-environment for the reduction of  $\text{TiO}_2$

**Table 1.** Reduction treatments to obtain the Magnéli phases

Reduction temperature(°C)	Heating/cooling Rate (°C/h)	Reduction duration (h)
800	150	24
900	150	24
1000	150	12
1100	150	12
1200	150	6
1300	150	1

### Microstructural characterisation

Density measurements were made on bulk samples, prepared with the same method as the fibres, using the Archimedes method described in the standard BS En623:2 [26]. Microstructural characterization was undertaken using X-ray diffraction (XRD, Philip PW1730, Cu-K $\alpha$ ,  $\lambda=1.541838\text{\AA}$ , 40kV, 25mA) and a Scanning Electron Microscope (SEM, JEOL JSM6480LV). Grain size analysis was conducted on the whole cross section of the fibres using the 'ImageJ' image analysis tool which involved (i) calibration of image dimensions, (ii) adjusting the threshold to observe the grain boundaries and (iii) determining the grain size using the particle size analysis tool of ImageJ. For the fibres sintered at 1300 °C thresholding was not possible to separate grain boundaries so each grain was individually measured in ImageJ.

### Electrical characterisation

The ac conductivity was determined for 1 to 10<sup>5</sup> Hz using a Solartron 1260 Impedance Analyser with a Solartron 1296 Dielectric Interface. In order to perform the electrical measurements electrical connections were attached to the ends of 260 $\mu\text{m}$  diameter fibres. In order to ensure ohmic electrical contacts linearity measurements were initially made using Pt, Ag and Al electrodes on multiple fibres. The Pt electrode was fired at 600°C, the Ag at 610°C and the Al at 670°C.

### Results and discussion

Figure 4a shows the XRD patterns for the sintered stoichiometric  $\text{TiO}_2$  fibres and the fibres carbo-thermally reduced at 800-1000°C. At these reduction temperatures the predominant phase is rutile; however a wide peak is present at approximately 24° that is characteristic of the Magnéli phases and indicates the presence of a purely crystalline phase of Ti-sub oxides. The colour of fibres is also indicative of these phase changes, since there is a colour change from yellowish ( $\text{TiO}_2$  fibres) to grey [27]. The fibres reduced at 1200°C and 1300°C had a bluish/black colour that is characteristic of the Magnéli phases and the XRD patterns (Figure 4b) confirm the presence of  $\text{Ti}_4\text{O}_7$  that is the most conductive of Magnéli phases.

The presence of a broad peak at  $2\theta$  of 20-30° is indicative of the presence of an amorphous phase. Diffuse diffraction peaks at 20-35° has been previously reported for sub-stoichiometric titania formed by laser irradiation [28]; which may lead to inferior chemical stability compared to well-crystallized oxides. Annealing was found to improve the crystallinity and conductivity 1-10 S/m [28], although the conductivity for the fibres reported in this paper are higher.

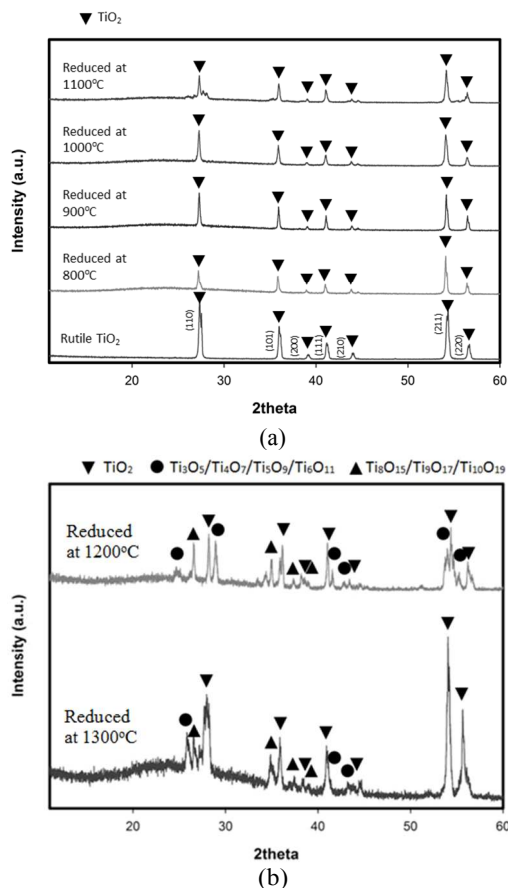


**Figure 4.** XRD patterns for (a)  $\text{TiO}_2$  and fibres reduced at 800–1100°C and (b) fibres reduced at 1200°C and 1300°C.

Figure 5 shows the high-density microstructure of the stoichiometric  $\text{TiO}_2$  fibres with an initial small grain size of 3.6  $\mu\text{m}$ . Figure 6 shows the reduced fibres that have been subject to carbo-thermal treatment at all temperatures in Table 1; indicating a high density and no micro-cracks due to the reduction process. This is also confirmed by the density measurements conducted on the bulk samples, as shown in Table 2. The reduction at high temperatures (1200°C and 1300°C) leads to significant grain growth with grain sizes up to 100  $\mu\text{m}$  for the higher temperature reduction process, see Table 3 and Figure 6.

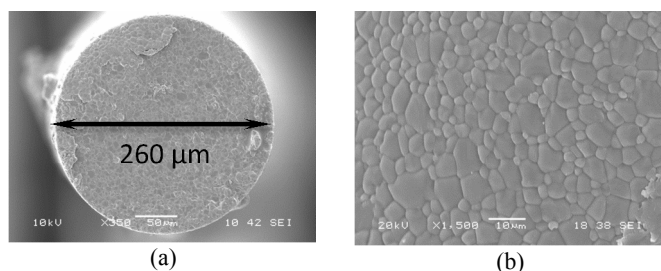


**Figure 5.** SEM of (a)  $\text{TiO}_2$  fibre, (b) microstructure

**Table 2.** Density of  $\text{TiO}_2$  and Magnéli phase bulk samples.

Sample	Theoretical density [11] ( $\text{g}/\text{cm}^3$ )	Bulk density ( $\text{g}/\text{cm}^3$ )	% Apparent solid porosity	%Theoretical density
$\text{TiO}_2$	4.23	4.17±0.20	0.24±0.05	98.65±0.48

Magnéli phase	4.3	4.16±0.07	3.04±0.62	96.65±1.65
---------------	-----	-----------	-----------	------------

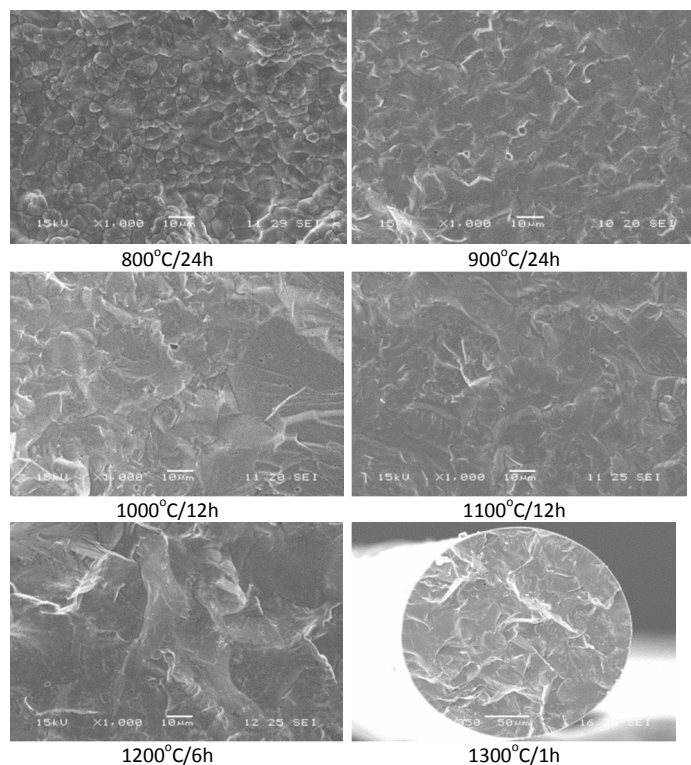


**Figure 6.** Microstructure of the reduced fibres

**Table 3.** Grain size of the fibres reduced at various temperatures calculated from the SEM images using ImageJ across the whole fibre cross-section of the fibres.

Fibre	Grain size ( $\mu\text{m}$ )
$\text{TiO}_2$	3.6
Reduced 800°C /24h	4
Reduced 900°C/24h	10-20
Reduced 1000°C/12h	50
Reduced 1100°C/12h	50
Reduced 1200°C/6h	70
Reduced 1300°C/1h	100

In order to ensure ohmic contacts for electrical characterisation Pt, Ag and Al electrodes were placed at the ends of 5 mm long fibres. Figure 7 shows the current-voltage (I-V) linearity measurements for each electrode type. Figure 7 shows that the most consistent I-V and linear (ohmic behaviour) response between fibres were achieved using Al electrodes; these were used for further characterisation. Non-ohmic behaviour is observed for Pt and Ag. Non-ohmic electrode contacts to semiconducting oxides are a well-known phenomenon where Schottky barriers develop at the metal-semiconductor interface due to mismatch in the Fermi energy levels of the sample and electrode metal [29]. Pt and Ag are common electrode materials for characterisation of low conductivity ceramic materials where non-ohmic behavior is not an issue. In the case of Magnéli phases the electrode selection is important for characterization of the material and ensuring ohmic contacts in the final device.

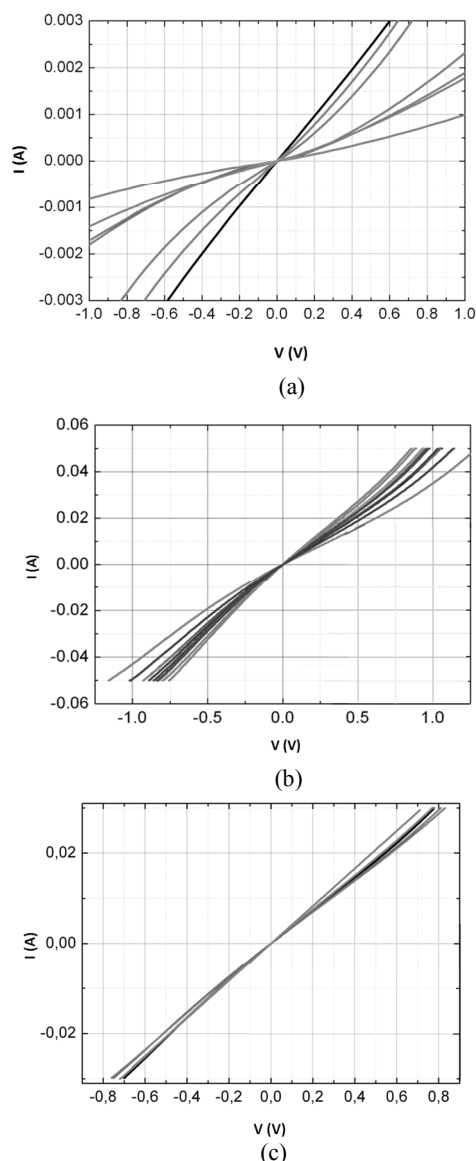


**Figure 7.** Linearity measurements (a) Pt, (b) Ag and (c) Al electrodes

The low frequency (100Hz) electrical conductivity of the fibres are shown in Figure 8. The sintered rutile  $\text{TiO}_2$  fibres are highly insulating with a conductivity of  $\sim 10^{-9}$  S/m. The reduced Ti-suboxide fibres reduced at 800-1100°C have an increased conductivity between  $10^{-1}$  - 10 S/m. It is also clear the samples reduced at 1200°C and 1300°C have metallic conductivity between  $10^3$ - $10^4$  S/m. For the reduced samples it was possible to tune the conductivity in a range of five orders of magnitude ( $10^{-1}$ - $10^4$  S/m) and the increase in electrical conductivity was  $10^{13}$  relative to the initial  $\text{TiO}_2$  fibres ( $\sim 10^{-9}$  S/m). From the low frequency measurements it is also clear that it is difficult to obtain consistent conductivity in the samples reduced at lower temperature, possibly due to the fact that the reduction process is slower at lower temperatures and it is more difficult to obtain a homogenous degree of reduction through the fibres. A great consistency in the conductivity of the fibres was observed for those reduced at 1200°C and 1300°C; see Figure 8.

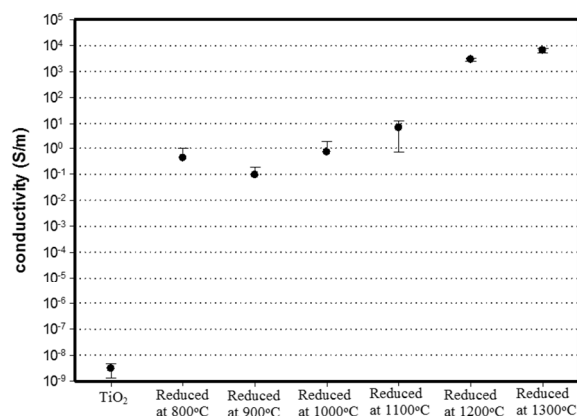


**Figure 8.** Low frequency electrical conductivity of  $\text{TiO}_2$  fibres and fibres reduced at various temperatures.

Measurements at a wider range of frequencies (1- $10^5$  Hz) were also conducted for the fibres reduced at 1200°C and 1300°C and the results shown in Figure 9a. It is clear that the Magnéli fibres are behaving as a conductor since its conductivity is frequency independent across the frequency range examined. The high conductivity and frequency independent behaviour also confirm that no insulating layer of TiC is likely to have developed, since a higher reduction temperature is required [30]. The initial  $\text{TiO}_2$  in Figure 9a is insulating and behaves as a dielectric with a frequency dependent conductivity ( $\sigma_{ac}$ ) with a gradient of unity, since  $\sigma_{ac} \sim \omega \cdot \pi \cdot f \cdot \epsilon$  where  $f$  is frequency and  $\epsilon$  is the permittivity of the fibre. These observations are also confirmed in Figure 9b where the fibres reduced at 1200°C and 1300°C exhibit a phase angle approaching  $0^\circ$  (as with a pure resistor/conductor) and the  $\text{TiO}_2$  fibres have a phase angle close to  $90^\circ$  (capacitive behaviour).

## Conclusions

A variety of high conductivity titanium sub-oxide fibres, including Magnéli phases ( $\text{Ti}_n\text{O}_{2n-1}$ ,  $3 < n < 10$ ) have been prepared by reducing rutile  $\text{TiO}_2$  in a carbon black micro-environment. The manufacturing process developed is able to produce dense (>96%) conductive fibres. Various reduction temperatures and durations have been tested and the extent of reduction was estimated using XRD and SEM and by measuring the electrical properties. The process is able to tune the conductivity of reduced fibres by five orders of magnitude ( $10^{-1}$  -  $10^4$  S/m) and increase the conductivity by  $10^{13}$  compared to the  $\text{TiO}_2$  material. Magnéli fibres that were reduced at 1200°C and 1300°C provided the most consistent and highest electrical conductivity. It was confirmed by the XRD that at these temperatures the  $\text{Ti}_4\text{O}_7$  phase is formed which is the most conductive of the Magnéli phases. These novel fibres will have potential use as a sensing element, electrode, catalyst support and energy storage applications.



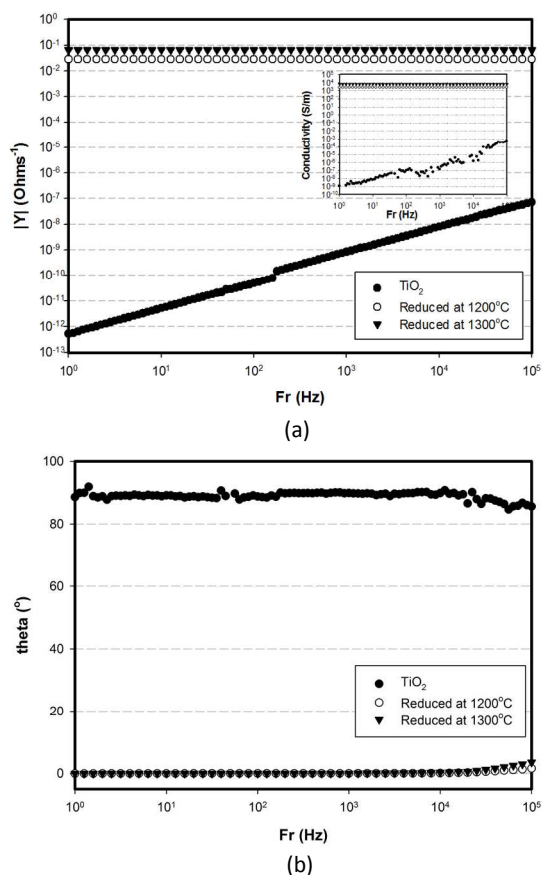


**Figure 9.** (a) Modulus of conductivity of TiO<sub>2</sub> fibres and fibres reduced at 1200°C and 1300°C over a range of frequencies. Inset shows real part of ac conductivity with frequency, (b) Phase angle of TiO<sub>2</sub> fibres and fibres reduced at 1200°C and 1300°C over a range of frequencies.

## Acknowledgements

The research leading to these results was funded by the European Union Seventh Framework Programme (FP7/20072013) under grant agreement no CP-TP 229099–2 as part of the ‘MesMesh’ project. Prof. Bowen acknowledges funding from the European Research Council under the European Union's Seventh Framework Programme (FP/2007-2013) / ERC Grant Agreement no. 320963 on Novel Energy Materials, Engineering Science and Integrated Systems (NEMESIS).

## Notes and references

<sup>a</sup> Materials Centre, Department of Mechanical Engineering, University of Bath (UK).

<sup>b</sup> High Performance Ceramics, EMPA Materials Science and Technology, Zurich (CH).

<sup>c</sup> Chemistry Department, Centre for Physical Sciences & Technology, Vilnius (LT).

<sup>d</sup> Department of Electronic and Electrical Engineering, University of Bath (UK).

1. S. Andersson, A. Magneli, *Naturwissenschaften*, 1956, 43, 495.
2. J. Nowotny, T. Bak, M.K. Nowotny, L.R. Sheppard, *International Journal of Hydrogen Energy*, 2007, 32, 2630.

3. G. Pfaff, P. Reynders, *Chemical Reviews*, 199, 99, 1963.
4. R. Vannoort, *Journal of Materials Science*, 1987, 22, 3801-3811.
5. M. A. Bañares, *Advanced Materials*, 2011, 23, 5293.
6. G. Chen, C. C. Waraksa, H. Cho, D. D. Macdonald, T. E. Mallouka, *Journal of The Electrochemical Society*, 2003, 150, E423.
7. M. A. Fox, M.T. Dulay, *Chemical Reviews*, 1993, 93, 341.
8. A. Fujishima, K. Honda, *Nature*, 1972, 238, 37.
9. L. Li, X. Liu, Y. Zhang, P. A. Salvador, G. S. Rohrer, *Int. J. Hydrogen Energy* 2013, 38, 6948.
10. L. Li, G. S. Rohrer, P. A. Salvador, *J. Am. Ceram. Soc.* 2012, 95, 1414.
11. B. Oregan, M. Gratzel, *Nature*, 1991, 353, 737.
12. G. Korotcenkov, *Materials Science and Engineering B-Solid State Materials for Advanced Technology*, 2007, 139, 1.
13. P. C. S. Hayfield, ed. *Development of a New Material - Monolithic Ti<sub>4</sub>O<sub>7</sub> Ebonex Ceramic*. 2002, Royal Society of Chemistry, Thomas Graham House: Cambridge.
14. E. G. Seebauer, M.C. Kratzer, *Materials Science and Engineering: R: Reports*, 2006, 55, 57.
15. S. Harada, K. Tanaka, H. Inui, *Journal of Applied Physics*, 2010, 108, 0837031.
16. L. Liborio, N. Harrison, *Physical Review B*, 2008, 77, 104104.
17. F. C. Walsh, R.G.A. Wills, *Electrochimica Acta*, 2010, 55, 6342.
18. J. R. Smith, F.C. Walsh, R.L. Clarke, *Journal of Applied Electrochemistry*, 1998, 28, 1021.
19. A. Kitada, G.Hasegawa, Y.Kobayashi, K. Kanamori, K. Nakanishi, H. Kageyama, *Journal of the American Chemical Society*, 2012, 134, 10894.
20. X. Li, A. L. Zhu, W. Qu, H. Wang, R. Hui, L. Zhang, J. Zhang, *Electrochimica Acta*, 2010, 55, 5891.
21. C. Yao, F. Li, X. Li, D. Xia, *Journal of Materials Chemistry*, 2012, 22, 16560.
22. A.Kitada, G. Hasegawa, Y. Kobayashi, K. Miyazaki, T. Abe, K. Kanamori, K. Nakanishi, H. Kageyama, *RSC Advances*, 2013, 3, 7205.
23. M. Canillas, E. Chinarro, M. Carballo-Vila, J. R. Jurado, B. Moreno, *Journal of Materials Chemistry B*, 2013, 1, 6459.
24. S. Myung, M. Kikuchi, C. S. Yoon, H. Yashiro, S. Kim, Y. Sun, B. Scrosati, *Energy & Environmental Science*, 2013, 6, 2609.
25. J. Heiber, T. Graule, D. Hulsenberg, *Advanced Engineering Materials* 2005, 7, 404.
26. BSI, *Advanced technical ceramics — Monolithic ceramics — General and textural properties in Part 2: Determination of density and porosity*. 1993, BSI 10-1999.
27. F. C. Walsh, R.G.A. Wills, *Electrochimica Acta*, 2010, 55, 6342.
28. T. Ioroi, H. Kageyama, T. Akita, K. Yasuda, *Phys. Chem. Chem. Phys.*, 2010, 12, 7529.
29. M. C. Ferrarelli, D. C. Sinclair, A. R. West, H. A. Dabkowska, A. Dabkowski, G. M. Luke, *J. Mat. Chem.*, 2009, 19, 5916
30. W. Sen, H. Sun, B. Yang, B. Xu, W. Ma, D. Liu, Y. Dai, *International Journal of Refractory Metals and Hard Materials*, 2010, 28, 628.